A Study of the Mechanism of Iron Carbonyl-Catalyzed Isomerization of 1-Pentene in the Gas Phase Using Time-Resolved Infrared Spectroscopy

Gregory T. Long† and Eric Weitz*

Contribution from the Department of Chemistry, Northwestern University, Evanston, Illinois 60208-3113

Received May 3, 1999

Abstract: After generation of $Fe(CO)_3$ by 308-nm gas-phase photolysis of $Fe(CO)_5$, 1-pentene adds to $Fe(CO)_3$ to form $Fe(CO)_3(\eta^2$-1-pentene) with a bimolecular rate constant of $k_a = (4 \pm 1) \times 10^{-10}$ cm^3 molecule^{-1} s^{-1}. Rapid β-hydrogen transfer, by way of intramolecular C−H bond insertion to form $HFe(CO)_3(\eta^3$-$C_5H_9)$, follows rate-limiting addition of 1-pentene to $Fe(CO)_3$ and proceeds with a lower bound of $k_1 \geq 10^9$ s^{-1}. Under experimental conditions, $HFe(CO)_3(\eta^3$-$C_5H_9)$ decays on a millisecond time scale with concurrent formation of $Fe(CO)_3(\eta^2$-pentene$)_2$ by addition of 1-pentene to an $Fe(CO)_3(\eta^2$-pentene) intermediate. It is $Fe(CO)_3(\eta^2$-pentene) that is in equilibrium with $HFe(CO)_3(\eta^3$-$C_5H_9)$ that adds 1-pentene to form $Fe(CO)_3(\eta^2$-pentene$)_2$, which may contain an isomerized olefin. CO may add to $Fe(CO)_3(\eta^2$-pentene) that is in equilibrium with $HFe(CO)_3(\eta^3$-$C_5H_9)$ to form $Fe(CO)_4(\eta^2$-pentene). $Fe(CO)_4(\eta^2$-pentene) remains stable on the time scale of catalytic turnover and its formation serves as a termination pathway for thermal catalysis. This system is compared to the analogous propene system (Long, G. T.; Wang, W.; Weitz, E. *J. Am. Chem. Soc.* **1995**, *117*, 12810). The major difference in behavior between these systems is attributed to an ∼3 orders of magnitude shift in the equilibrium constant toward $HFe(CO)_3(\pi$-allyl) relative to $Fe(CO)_3$(olefin) when the starting olefin is 1-pentene instead of propene. The magnitude of the equilibrium constants indicates that there is an ∼4 kcal mol^{-1} greater enthalpy difference between $HFe(CO)_3(\eta^3$-$C_5H_9)$ and $Fe(CO)_3(\eta^2$-pentene) than for the corresponding species in the propene system.

I. Introduction

Metal carbonyls are a well-studied and well-characterized class of organometallic compounds.[1−5] Their photolability, by near-UV light, as well as the thermal lability of ligands in many compounds, allows for facile generation of coordinatively unsaturated metal carbonyls. These reactive species can catalyze a variety of reactions such as olefin isomerization, olefin hydrogenation, hydroformylation, and hydrosilation.[1−5]

Iron pentacarbonyl is a particularly well-investigated metal carbonyl that has been the focus of a wide variety of both thermal and photochemical studies of transition metal-catalyzed olefin isomerization. Some relevant studies are cited in refs 6−15. The mechanism that is now generally accepted for iron pentacarbonyl-induced isomerization of olefins is shown in Scheme 1 and involves an $Fe(CO)_3$(olefin) complex. Once this species is generated, either by photochemical or thermal processes, a β-hydrogen transfer process, which can be quite facile, can lead to formation of a π-allyl hydride. Reversion of this species back to a monoolefin adduct can be accompanied by isomerization of the olefin. Formation of a labile bisolefin complex can occur by addition of olefin to the monoolefin adduct. Loss of the isomerized olefin from this bisolefin species will regenerate the monoolefin complex and lead to reentry of $Fe(CO)_3$(olefin) into the catalytic cycle.

Scheme 1

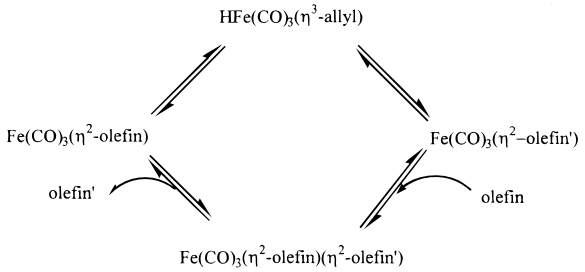

† Department of Chemistry, University of Utah, Salt Lake City, UT 84112.

(1) Collman, J. P.; Hegedus, L. S.; Norton, J. R.; Finke, R. G. *Principles and Applications of Organotransition Metal Chemistry*, 2nd ed.; University Science Books: Mill Valley, CA 1987.

(2) Jordan, R. B. *Reaction Mechanisms of Inorganic and Organometallic Systems*; Oxford University Press: New York, 1991.

(3) Crabtree, R. H. *The Organometallic Chemistry of the Transition Metals*; Wiley-Interscience: New York, 1994.

(4) Geoffroy, G. L.; Wrighton, M. S. *Organometallic Photochemistry*; Academic Press: New York, 1979.

(5) Atwood, J. D. *Inorganic and Organometallic Reaction Mechanisms*; Brooks/Cole: Monetrey, CA, 1985.

(6) Casey, C. P.; Cyr, C. R. *J. Am. Chem. Soc.* **1973**, *95*, 2248.

(7) Fleckner, H.; Grevels, F.-W.; Hess, D. *J. Am. Chem. Soc.* **1984**, *106*, 2027.

(8) Schroeder, M. A.; Wrighton, M. S. *J. Am. Chem. Soc.* **1976**, *98*, 551.

(9) Chase, D. B.; Weigert, F. J. *J. Am. Chem. Soc.* **1981**, *103*, 977.

(10) Mitchner, J. C.; Wrighton, M. S. *J. Am. Chem. Soc.* **1981**, *103*, 975.

(11) Whetten, R. L.; Fu, K.-J.; Grant, E. R. *J. Am. Chem. Soc.* **1982**, *104*, 4270.

(12) Fu, K.-J.; Whetten, R. L.; Grant, E. R. *Ind. Eng. Chem. Res. Dev.* **1984**, *23*, 33.

(13) Mitchner, J. C.; Wrighton, M. S. *J. Am. Chem. Soc.* **1983**, *105*, 1065.

(14) Barnhart, T. M.; McMahon, R. J. *J. Am. Chem. Soc.* **1992**, *114*, 5434.

(15) Whetten, R. L.; Fu, K.-J.; Grant, E. R. *J. Chem. Phys.* **1982**, *77*, 3769.

10.1021/ja9914341 CCC: $19.00
Published on Web 02/05/2000

The details of this cycle and related catalytic processes have been of great interest and have motivated a variety of studies of these and similar systems. For example, the lability of the cyclooctene ligands in $Fe(CO)_3(\eta^2$-*cis*-cyclooctene$)_2$ make it a quantitative "synthetic" source of $Fe(CO)_3$ because the cyclooctene moieties undergo facile thermal substitution by 1-pentene which results in extensive isomerization with turnover numbers up to 2000.[7] In a revealing study of the thermal isomerization of 3-ethyl-1-pentene-*3*-d_1, Cyr and Casey showed by NMR scrambling experiments that isomerization proceeds by intramolecular 1,3-hydrogen shifts.[6]

As indicated, photolysis can be another method to produce coordinatively unsaturated intermediates.[5] Using extended continuous photolysis of an olefin/$Fe(CO)_5$ mixture, Schroeder and Wrighton showed that any one of the linear pentenes isomerizes to the thermodynamic ratio with a quantum yield approaching 500.[8] In an in situ FTIR investigation of 1-pentene isomerization induced by continuous UV irradiation, Chase and Weigert followed the spectroscopic changes associated with intermediates that occurred during irradiation and the termination of isomerization after irradiation.[9]

Pulsed photolysis allows for the study of reactions in a catalytic cycle under thermal conditions between the laser pulses that generate coordinatively unsaturated species and initiate a catalytic cycle. Grant and co-workers measured the rate of net isomerization and reported turnover numbers of 4000 s^{-1} for the pulsed photolysis of iron pentacarbonyl in neat 1-pentene.[11] In a related investigation, their analysis of the isomerization cycle indicated their results were compatible with the mechanism shown in Scheme 1.[12] They reported catalytic turnover rates of $\sim 10^4$ s^{-1} and an activation energy of $\sim$2.8 kcal mol^{-1} for the rate-limiting step in the catalytic cycle.

Matrix isolation has proven very valuable in identifying and spectroscopically characterizing proposed intermediates in iron carbonyl-catalyzed olefin isomerization. Photolyzing $Fe(CO)_4$(olefin) in a methylcyclohexane (MCH) matrix at 77 K, Mitchner and Wrighton observed the formation of $Fe(CO)_3$(olefin) for olefins without β-H's (olefin = ethylene, 3,3-dimethyl-1-pentene) and $HFe(CO)_3(\pi$-allyl) for olefins with β-H's (olefin = propene, 1-pentene).[13] When Barnhart and McMahon photolyzed $Fe(CO)_4(\eta^2$-$C_3H_6)$ in Ar and MCH matrices at 10 K, they observed both $Fe(CO)_3(\eta^2$-$C_3H_6)$ and $HFe(CO)_3(\eta^3$-$C_3H_5)$.[14] Further, at 5 K they observed the thermal conversion of $Fe(CO)_3(\eta^2$-$C_3H_6)$ to $HFe(CO)_3(\eta^3$-$C_3H_5)$, showing the latter to be thermodynamically more stable.

Laser flash photolysis coupled with time-resolved IR spectroscopy provides a powerful method for studying reaction intermediates and pathways in real time.[16−27] The considerable infrared extinction coefficients of the CO ligands provide for a convenient spectroscopic probe of these species that potentially allows for direct monitoring of reaction intermediates.[4,17] The sensitivity of the M−(C−O) infrared stretching frequencies to the environment surrounding the metal center makes this a structure-sensitive probe.[17] This technique has been applied to study the reactive behavior of metal carbonyls and for measurements of the kinetics and energetics of systems of ligands weakly bound to metal carbonyls.[28] In addition, it has been shown that in the gas phase an increase in the energy of the photolysis photon generally leads to the production of more highly coordinatively unsaturated metal carbonyls.[29,30] In the context of Scheme 1, the ability to produce $Fe(CO)_3$ in a single photolysis step provides conditions under which this species can react with olefin and directly enter into the catalytic cycle. The method of pulsed generation of the starting coordinatively unsaturated species also facilities studies of the details of the kinetics and mechanism of olefin isomerization.

Transient infrared spectroscopy has recently been used to determine the kinetics and energetics for the $Fe(CO)_5$/propene system in which a π-allyl metal hydride, $HFe(CO)_3(\eta^3$-$C_3H_5)$, invoked as a key intermediate in olefin isomerization, was characterized.[16] That study either measured or provided an estimate for the rate constants and energetics of each step in the proposed catalytic cycle in Scheme 1. The current study of the $Fe(CO)_5$/1-pentene system is complimentary in that isomerization can occur and lead to production of the more thermodynamically favored *cis*- and *trans*-2-pentene isomers. In addition, the generality of the mechanism and the kinetics deduced in this prior study can be evaluated and the effect of chain length on the microscopic kinetics and thermodynamics of the system can be assessed.

II. Experimental Section

The experimental apparatus used in this study has been described in detail elsewhere.[16,17,31,32] Briefly, experiments were performed in either a flow cell or a static cell, both made of Pyrex and terminated by CaF_2 windows. In flow experiments, calibrated mass flow controllers regulated the flow of ligand and buffer gases to a 35 × 1.5 cm (i.d.) flow cell. A needle valve metered the $Fe(CO)_5$ and its pressure was determined from its absorbance. Capacitance manometers measured the pressure of sample gases delivered to a 42 × 2.5 cm (i.d.) static cell.

This study used two infrared probes. Reactions occurring on either a microsecond or millisecond time scale were monitored by a tunable diode laser. The diode laser beam double-passed the cell and a fast InSb detector monitored the absorption of radiation by photoproducts. The response time of the detector was determined to be $\sim$70 ns from single-exponential fits of the detector-limited photolytic decay of $Fe(CO)_5$. The detector output was amplified, digitized, and signal averaged before being stored on a PC for data manipulation. Time-resolved spectra with four wavenumber resolution were constructed by connecting transient waveforms that spanned the spectral region of interest

(16) Long, G. T.; Wang, W.; Weitz, E. *J. Am. Chem. Soc.* **1995**, *117*, 12810.
(17) Weitz, E. *J. Phys. Chem.* **1987**, *91*, 3945.
(18) George, M. W.; Polaikoff, M.; Turner, J. J. *Analyst* **1994**, *119*, 551.
(19) Wang, W.; Jin, P.; Liu, Y.; She, Y.; Fu, K.-J. *J. Phys. Chem.* **1992**, *96*, 1278.
(20) Fletcher, T. R.; Rosenfeld, R. N. *J. Am. Chem. Soc.* **1988**, *110*, 2097; **1985**, *107*, 2203.
(21) Breheny, C. J.; Draper, S. M.; Grevels, F. W.; Klotzbucher, W. E.; Long, C.; Pryce, M. T.; Russell, G. *Organometallics* **1996**, *15*, 3679.
(22) Ishikawa, Y.; Arai, S. *Chem. Phys. Lett.* **1996**, *253*, 230.
(23) Colombo, M.; George, M. W.; Moore, J. N.; Pattison, D. I.; Perutz, R. N.; Virrels, I. G.; Ye, T. Q. *J. Chem. Soc., Dalton Trans.* **1997**, *17*, 2857.
(24) Sprague, J. R.; Arrivo, S. M.; Spears, K. G. *J. Phys. Chem.* **1991**, *95*, 10528.
(25) Grubbs, W. T.; Dougherty, T. P.; Heilweil, E. J. *Chem. Phys. Lett.* **1994**, *227*, 480.
(26) (a) Bromberg, S. E.; Yang, H.; Asplund, M. C.; Lian, T.; McNamara, B. K.; Kotz, K. T.; Yeston, J. S.; Wilkens, M.; Frei, H.; Bergman, R. G.; Harris, C. B. *Science* **1997**, *278*, 260. (b) Yang, H.; Kotz, K. T.; Asplund, M. C.; Wilkens, M. J.; Harris, C. B. *Acc. Chem. Res.* **1999**, *32*, 551. (c) McNamara, B. K.; Yeston, J. S.; Bergman, R. G.; Moore, C. B. *J. Am. Chem. Soc.* **1999**, *121*, 6437.
(27) McFarlane, K.; Lee, B.; Bridgewate, J.; Ford, P. C. *J. Organomet. Chem.* **1998**, *554*, 49.
(28) (a) House, P. G.; Weitz, E. *J. Phys. Chem. A* **1997**, *101*, 2988. (b) Wells, J. R.; House, P. G.; Weitz, E. *J. Phys. Chem.* **1994**, *98*, 8343.
(29) (a) Rayner, D. M.; Ishikawa, Y.-I.; Brown, C. E.; Hackett, P. A. *Laser Chemistry of Organometallics*; Chaiken, J., Ed., ACS Symp. Ser. No. 530; American Chemical Society: Washington, DC, 1993; p 96. (b) Ishikawa, Y.-I.; Brown, C. E.; Hackett, P. A.; Rayner, D. M. *J. Phys. Chem.* **1990**, *94*, 2404.
(30) Ryther, R. J.; Weitz, E. *J. Phys. Chem.* **1992**, *96*, 2561.
(31) Weitz, E. *J. Phys. Chem.* **1994**, *98*, 11256.
(32) Poliakoff, M.; Weitz, E. *Adv. Organomet. Chem.* **1986**, *25*, 277.

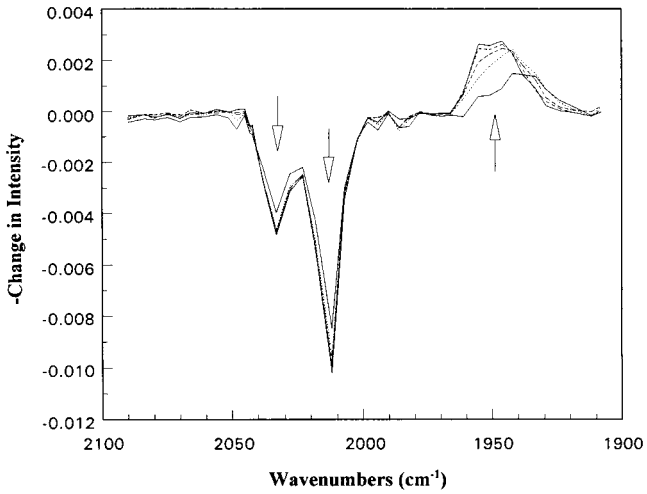

Figure 1. A time-resolved diode laser flow cell spectrum of ~50 m Torr of $Fe(CO)_5$ in the presence of 3 Torr of helium generated by 308-nm photolysis. The spectrum displays the time interval in 0.5 μs increments from 0.5 to 2.5 μs after the photolysis pulse. The first and last time increments are solid traces and the arrows indicate the direction of evolution of the absorptions over this time interval.

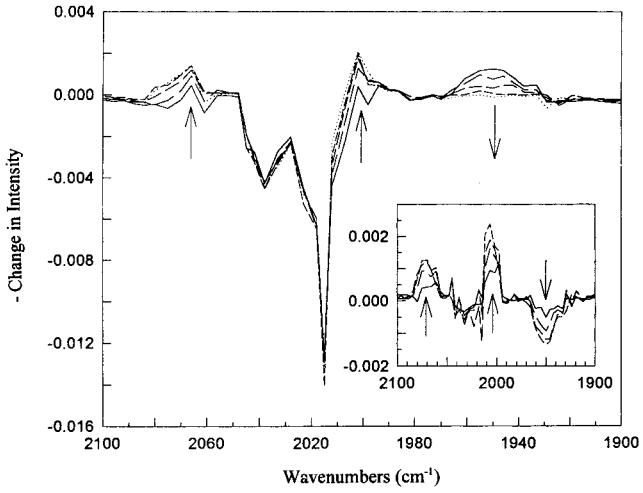

Figure 2. A time-resolved IR diode laser flow cell spectrum of ~50 mTorr of $Fe(CO)_5$, 489 mTorr of 1-pentene, and the balance He up to a total pressure of 12.1 Torr. The spectrum was collected over a time scale of 0.2−1.4 μs and is shown in increments of 0.3 μs. The solid line is the first trace and the arrows show the progression of the spectral features. The inset shows a difference spectrum generated by subtracting subsequent spectra from the first one.

at common delay times. Reactions occurring on time scales of minutes or longer were followed with a time-resolved FTIR spectrometer. The "GC" mode of the FTIR is most conveniently used to monitor processes taking place on a time scale of hundreds of milliseconds or longer.

When using the diode laser probe, the photolysis source consisted of the unfocused 308-nm output of an excimer laser running on XeCl. When probing by FTIR spectroscopy, the 355-nm radiation generated by a frequency-tripled Nd:YAG laser was employed. For both systems typical fluences of ~7 mJ cm^{-2} were measured at the front cell window. At these fluences the photolysis of $Fe(CO)_5$ has been shown to be dominated by a single photon process.[33,34]

Reaction kinetics were monitored by collecting transient waveforms at frequencies of interest as a function of reactant pressure and sample temperature. Transient waveforms were fit to exponentials using Scientist[35] or Mathcad[36] software. Unless otherwise stated, all rate constants were measured at 296 ± 2 K with an assigned error of 2σ as determined by linear regression.

For experiments above room temperature, the temperature of the cell was varied over a range of 296−318 K by wrapping a cardboard shroud, which encompassed the cell, with heating tape. The use of the shroud facilities temperature uniformity along the length of the cell, which was monitored by thermocouples placed at the center and ends of the cell and had an estimated uncertainly of ±1 K.

Experiments directed toward the measurement of the rate constant for formation of $HFe(CO)_3(C_5H_9)$ used 50 mTorr of $Fe(CO)_5$, 25−300 mTorr of 1-pentene, and a balance of He up to a total pressure of 50 Torr. The helium buffer gas acts as a collisional relaxer of excited vibrational and rotational states and as a "third body" in collisionally stabilizing association reactions, ensuring that reactions occur in the "high-pressure" limit.[17] Experiments to measure the decay of $HFe(CO)_3(C_5H_9)$ and the concomitant growth of $Fe(CO)_3(1\text{-pentene})_2$ used 100 mTorr of $Fe(CO)_5$ and 50−400 Torr of 1-pentene.

$Fe(CO)_5$ (Aldrich) was degassed prior to use and purified by several freeze−pump−thaw cycles. 1-Pentene (Aldrich; 99% pure) was also purified by freeze−pump−thawing. He (Linde; 99.999%) was used as received.

III. Results

As shown in Figure 1, the 308-nm photolysis of 50 mTorr of $Fe(CO)_5$ and 3 Torr of He gives rise to principally, if not exclusively, a single photoproduct, which can be identified as $Fe(CO)_3$ based on the position of the absorption at ~1950 cm^{-1}.[37] A prior report of the product yield after 308-nm photolysis of $Fe(CO)_5$ indicates that $Fe(CO)_3$ is clearly the dominant photoproduct.[29a] The $Fe(CO)_3$ absorption is centered at ~1940 cm^{-1} in the first transient spectrum after photolysis. The sharpening and blue shifting of the $Fe(CO)_3$ absorption that occurs over the first ~2 μs following photolysis is characteristic of the relaxation of an internally excited primary photoproduct.[17] As shown in Figure 2, when $Fe(CO)_5$ is photolyzed in the presence of ~500 mTorr of 1-pentene the spectrum changes considerably. The decay of the absorption due to $Fe(CO)_3$ is accompanied by the simultaneous formation of a species with infrared absorption bands at 2067 and 2000 cm^{-1}. This spectrum was collected over a time scale of 0.2−1.4 μs and is shown in increments of 0.3 μs. The contribution to the spectrum due to the depletion of $Fe(CO)_5$ can be removed by subtracting subsequent traces from the first one. When the subtraction spectrum, shown in the inset, is compared to the original spectrum it is clear that photolytic depletion of the overlapping parent absorption in the original spectrum obscured much of the lower frequency product band that now appears in the inset with a maxima at ~2006 cm^{-1}. The rate of appearance of the higher frequency band of species I, at 2067 cm^{-1}, which is not overlapped by an absorption band of $Fe(CO)_5$, was studied as a function of 1-pentene pressure under pseudo-first-order conditions. The slope of the plot of the rate of decay of $Fe(CO)_3$ at 1951 cm^{-1}, as a result of reaction of 1-pentene with $Fe(CO)_3$, yields a rate constant of $k = (5 \pm 2) \times 10^{-10}$ cm^3 $molecule^{-1}$ s^{-1}. The rate constant measured for formation of species I, at 2067 cm^{-1} (Figure 3), as a function of the pressure of 1-pentene, was $(4 \pm 1) \times 10^{-10}$ cm^3 $molecule^{-1}$ s^{-1}. These rate constants are within experimental error of each other and, as will be shown, formation of species I is rate-limited by the addition of 1-pentene to $Fe(CO)_3$. These rate constants are comparable to those measured for the addition of *cis*-2-pentene, *trans*-2-pentene, and propene to $Fe(CO)_3$[44a] and approach the gas kinetic rate constants for these systems of ~7×10^{-10} cm^3 $molecule^{-1}$ s^{-1}.[38]

(33) Waller, I. M.; Hepburn, J. W. *J. Chem. Phys.* **1988**, *88*, 6658.
(34) Nathanson, G.; Gitlin, B.; Rosan, A. N.; Yardley, J. T. *J. Chem. Phys.* **1981**, 74, 361.
(35) *Scientist*; MicroMath Scientific Software: Salt Lake City, UT, 1994.
(36) *Mathcad*; Mathsoft Inc.: Cambridge, MA, 1994.
(37) Ryther, R. J.; Weitz, E. *J. Phys. Chem.* **1991**, *95*, 9842.

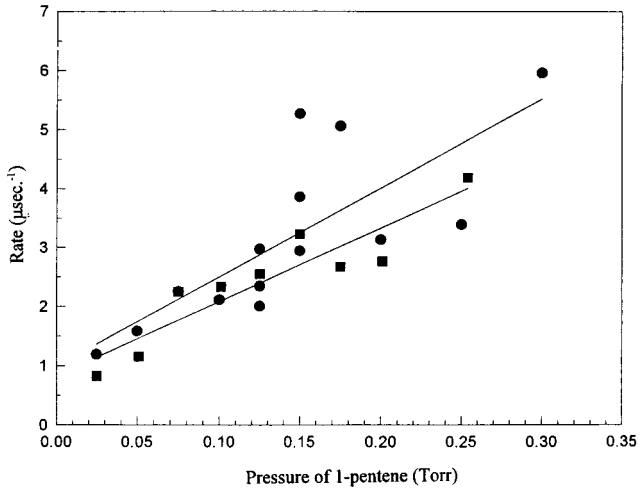

Figure 3. A plot of the pseudo-first-order rates of decay of $Fe(CO)_3$ at 1951 cm^{-1} (●) and the formation of Species I at 2067 cm^{-1} (■) measured at 296 K as a function of 1-pentene pressure.

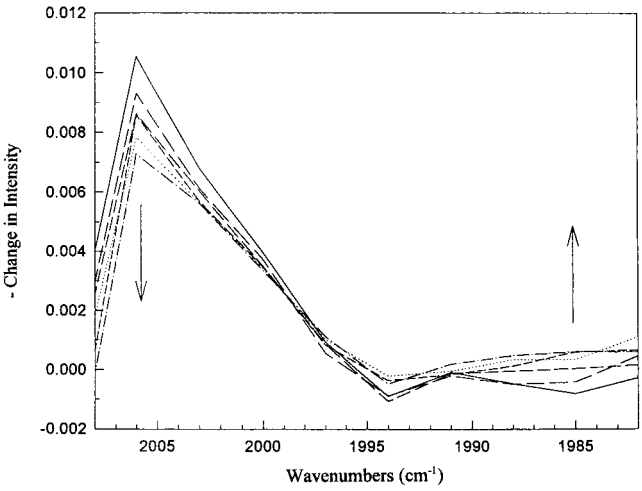

Figure 4. Time-resolved IR diode laser static cell spectrum of 100 mTorr of $Fe(CO)_5$ and 380 Torr of 1-pentene. The spectrum is shown over a time scale of 2−22 ms in increments of 4 ms. The solid line is the first trace and the arrows show the progression of the spectral features.

The absorption of species I at 2006 cm^{-1} decays on the millisecond time scale with concomitant formation of species II, with an absorption band at 1985 cm^{-1}. A time-resolved IR diode laser spectrum shown in Figure 4 illustrates this process for the 308-nm photolysis of a cell fill of 100 mTorr of $Fe(CO)_5$ and 380 Torr of 1-pentene. The absorption of a new species at 1985 cm^{-1}, though apparent in this spectrum, is even clearer in individual traces taken at this frequency. There also appears to be an isobestic point at ∼1998 cm^{-1} that is consistent with the conversion of species I to species II occurring by a direct process.

The rate of formation of species II was typically monitored at 1984 cm^{-1}. These signals are larger for higher pressures of 1-pentene and appear to be superimposed on either a sloping baseline or a slow exponential decay. This latter feature does not appear to vary significantly in amplitude with the pressure of 1-pentene. Thus, the signal due to species II is larger and better defined at higher 1-pentene pressures and the slower component of the signal makes analysis at lower pressures more

(38) Steinfeld, J. I.; Francisco, J. S.; Hase, W. L. *Chemical Kinetics and Dynamics*; Prentice Hall: Englewood Cliffs, NJ, 1989; Chapter 2.

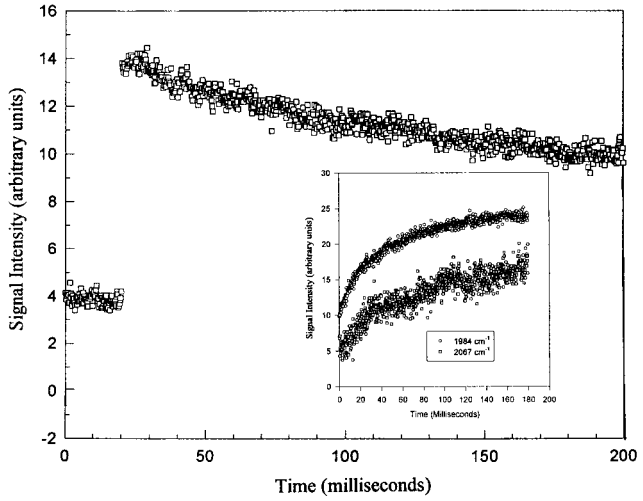

Figure 5. A transient waveform at 2067 cm^{-1} for a cell fill of 101 mTorr of $Fe(CO)_5$ and 400 Torr of 1-pentene (□). The inset displays a signal taken at 1984 cm^{-1} under comparable conditions and the falling portion of the 2067 cm^{-1} signal which has been inverted. The data have been scaled to facilitate a comparison of the signals.

difficult. However, within experimental error, the signals taken below 317.5 K, which are large enough to be successfully analyzed, have rates that have no systematic dependence on pentene pressure. For example, the rate of rise of species II for pressures of 200 and 401 Torr of 1-pentene, when fit as single exponentials, gives $k = 20.1 \pm 0.7$ and 21.6 ± 0.6 s^{-1}, respectively. For one data set taken at 317.5 K, the lower pressure curves analyzed to give rates that appeared to have a weak but monotonic dependence on 1-pentene pressure. However, when these curves were visually compared to higher pressure curves no pressure-dependent trend was apparent. We feel the variations in rate, obtained from the analysis program, is a result of the smaller signal-to-noise levels for the lower pressure, higher temperature data. There was no evidence in any of these data at any temperature for prompt formation of species II.

The signals due to species I, monitored at 2067 cm^{-1}, are more difficult to analyze than the signals at 1984 cm^{-1} since, as will be discussed in Section III.B.3, the amplitude of the 2067 cm^{-1} exponential decay is only a fraction of the total amplitude of the signal (see Figure 5). Analysis of these signals is also complicated by an apparent second, much more slowly decaying portion of the signal. Since the *amplitude* of the more rapidly decaying portion of the signal increases with increasing pressure of 1-pentene the best quality data are obtained at the highest pentene pressure. Nevertheless, even under these conditions the rates obtained from analysis of these signals have significant error brackets. However, as shown in the inset in Figure 5, a visual comparison of the fast decay at 2067 cm^{-1} and the rise of the 1984 cm^{-1} signal demonstrates that these processes have very similar rates. Though the signals at 2067 cm^{-1} degrade at lower pressures, as with the data at 1984 cm^{-1}, there is no apparent pressure dependence. As might be anticipated for such a situation, somewhat different rates are obtained from our analysis program for the data at these two wavelengths. This situation leads to activation energies for the process being monitored at both 2067 and 1984 cm^{-1} that differ in reported magnitude, but have overlapping error brackets (vide infra). The correspondence between the rate of the faster decay of species I and the rate of the rise of species II at 1984 cm^{-1} and the isobestic point at ∼1998 cm^{-1} support species I decaying to form species II. The slow decay that is seen at 2067 cm^{-1}

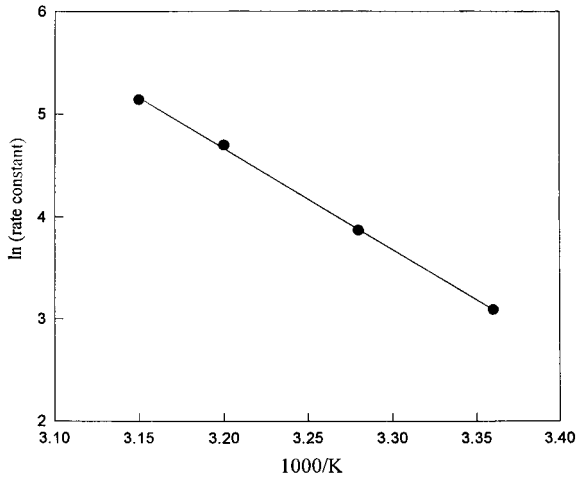

Figure 6. An Arrhenius plot for the rate of formation of Species II at 1984 cm^{-1}.

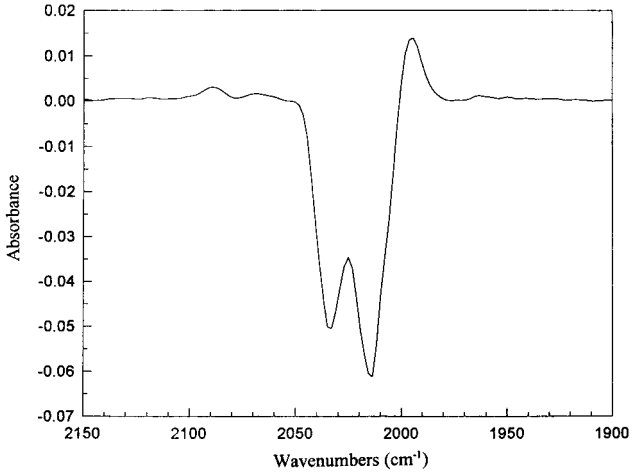

Figure 7. A gas-phase FTIR spectrum of Species III collected using 100 scans at 4 cm^{-1} resolution resulting from the 355-nm photolysis of a static cell fill of 100 mTorr of $Fe(CO)_5$ and 20 Torr of 1-pentene and a balance of He up to 50 Torr. The unphotolyzed cell was used as the reference.

could be due to limitations on the low-frequency response of the detection electronics or to a slow decay of species II.

The signals at 2006 cm^{-1}, assigned to species I, have a shape that is qualitatively similar to those at 2067 cm^{-1}. Less data were collected in this region since signals taken in this region could be perturbed by underlying absorptions due to $Fe(CO)_4$ and/or $Fe(CO)_5$. However, visual comparisons of better quality (higher pressure) signals taken at 2006 cm^{-1} gave good agreement with the rise rate of the signals at 1984 cm^{-1}, which are due to the growth of species II.

Though the rise rate of the absorption of species II at 1984 cm^{-1} is pressure independent over the range of pressures studied, it is temperature dependent. The rise rate increases as a function of temperature, as shown in an Arrhenius plot presented in Figure 6. The slope of this plot yields an activation energy of $E_a = 19.6 \pm 0.7$ kcal mol^{-1} and the *y*-intercept gives a preexponential factor of $A = 5.3 \times 10^{15}$ s^{-1}. The analogous activation energy for the decay of species I at 2067 cm^{-1}, $E_a = 16.3 \pm 5.3$ kcal mol^{-1}, agrees, within experimental error, with that obtained for species II at 1984 cm^{-1}.

The "GC" mode of the FTIR was employed to probe the behavior of the system on a longer time scale. To improve signal-to-noise, a transient population was built up with multiple laser pulses prior to the collection of spectra. A laser repetition rate of 4 Hz was used since higher repetition rates have been reported to lead to substrate turnover that becomes less than linear as a function of laser pulses, presumably due to the photolysis of catalytically active species.[15] A cell fill of 100 mTorr of $Fe(CO)_5$, 20 Torr of 1-pentene, and a balance of He up to 50 Torr total pressure was photolyzed for up to tens of minutes. On the time scale of the collection of "GC" FTIR spectra, obtained after photolysis, $Fe(CO)_5$, which has absorptions at 2035 and 2014 cm^{-1}, has been depleted and species III had already formed at 2089 and 1995 cm^{-1} (Figure 7). Photolysis also promotes isomerization as evidenced by the formation of 2-pentene (not shown). This observation of olefin isomerization is consistent with Whetten and co-worker's study of the isomerization of 1-pentene.[15] When they photolyzed a mixture of 1 Torr of $Fe(CO)_5$ and 340 Torr of 1-pentene over tens of minutes they observed isomerization to both *cis*- and *trans*-2-pentene.[15] In a related experiment, FTIR detection after 10 min of photolysis of a cell fill of 100 mTorr of $Fe(CO)_5$, 5 Torr of CO, 20 Torr of 1-pentene, and a balance of He up to 50 Torr total pressure resulted in a larger amplitude for the bands of species III than that for an analogous cell fill without added CO.

IV. Discussion

A. Microsecond Time Scale: Formation of Species I. 1. Assignment. The reaction of $Fe(CO)_3$ with 1-pentene leads to the formation of species I with gas-phase absorption bands at 2067 and 2006 cm^{-1}. Table 1 contains a compilation of the gas phase and matrix assignments of intermediates resulting from studies of the $Fe(CO)_5$/1-pentene and the $Fe(CO)_5$/propene systems. Reference to this table shows that the gas-phase bands of species I lie 8 and 17 cm^{-1} to higher frequency than the bands assigned to $HFe(CO)_3(\eta^3\text{-}C_5H_9)$, which are at 2059 and 1989 cm^{-1} in a MCH matrix. A shift of this magnitude is typical for an absorption band in the gas phase relative to the corresponding band in a matrix.[39]

Further, the positions of the absorptions and the behavior of species I are consistent with what has been observed for the π-allyl metal hydride complex formed in the $Fe(CO)_5$/propene system. The gas-phase absorptions of $HFe(CO)_3(\eta^3\text{-}C_3H_5)$ occur at 2080 and 2011 cm^{-1}, 13 and 5 cm^{-1} to higher energy than those of species I (Table 1). $HFe(CO)_3(\eta^3\text{-}C_3H_5)$ can form after the reaction of $Fe(CO)_3$ and propene as a result of a β-hydrogen transfer process. The net electron donating character of the larger pentyl moiety relative to the propyl moiety would be expected to result in greater σ-donation[1,3] in $HFe(CO)_3(\eta^3\text{-}C_5H_9)$ relative to $HFe(CO)_3(\eta^3\text{-}C_3H_5)$. The greater electron density on the metal would be expected to lead to greater back-donation into the CO antibonding orbitals, which leads to a weaker C−O bond that will be reflected in a red shift of the M−CO IR stretching frequency, as observed. Based on similarities with matrix work and the parallels with the analogous propene system, species I is assigned as $HFe(CO)_3(\eta^3\text{-}C_5H_9)$.

2. Mechanism. Thus, in the presence of 1-pentene, $Fe(CO)_3$ decays with concurrent formation of $HFe(CO)_3(\eta^3\text{-}C_5H_9)$. However, the rate for formation of $HFe(CO)_3(\eta^3\text{-}C_5H_9)$ *appears to* depend on the pressure of 1-pentene. As indicated, its rate of formation can be characterized by a bimolecular rate constant, $k_a = (4 \pm 1) \times 10^{-10}$ cm^3 $molecule^{-1}$ s^{-1}, as measured at 2067 cm^{-1}. Analogous behavior was observed with propene. A mechanism involving the rate-limiting addition of propene to $Fe(CO)_3$ and subsequent rapid β-hydrogen transfer leads to the apparent propene pressure dependence for the rise of $HFe(CO)_3(\eta^3\text{-}C_3H_5)$.

(39) Hllam, H. E., Ed. *Vibrational Spectroscopy of Trapped Species*; Wiley: New York, 1973.

Table 1[a]

$Fe(CO)_3(C_3H_6)$ (gas, 296 K)		16
$Fe(CO)_3(C_3H_6)_2$ (gas, 296 K)	2060, 1988	16
$Fe(CO)_3(C_3H_6)_2$ (MCH matrix, 90 K)	2051 (1.0), 1971 (11)	42
$Fe(CO)_3$(pentene) (gas, 296 K)		this study
$Fe(CO)_3$(pentene)$_2$ (gas, 296 K)	1985	this study
$Fe(CO)_3$(1-pentene)$_2$ (1-pentene, 195 K)	2048 (1.0), 1972 (16.6)	42
$HFe(CO)_3(C_3H_5)$ (gas, 296 K)	2080, 2011	16
$HFe(CO)_3(C_3H_5)$ (Ar matrix, 10 K)	2070 (1.0), 2004 (2.9), 2001 (2.3)	14
$HFe(CO)_3(C_5H_9)$ (gas, 296 K)	2067, 2006	this study
$HFe(CO)_3(C_5H_9)$ (MCH matrix, 90 K)	2059 (1.0), 1989 (1.5)	42
$Fe(CO)_4(C_3H_6)$ (gas, 296 K)	2089, 2014, 1988	16
$Fe(CO)_4(C_3H_6)$ (matrix, 10 K)	2088 (1.0), 2006 (3.7), 1986 (2.4)	14
$Fe(CO)_4$(pentene) (gas, 296 K)	2089, $\leq$1995[b]	this study
$Fe(CO)_4$(1-pentene) (3MP, 298 K)	2083 (1.0), 2002 (5.4), 1981 (4.2)	42

[a] MCH = methylcyclohexane; 3MP = 3-methylpentane. [b] See text in Section IV. C.1 for details.

Scheme 2

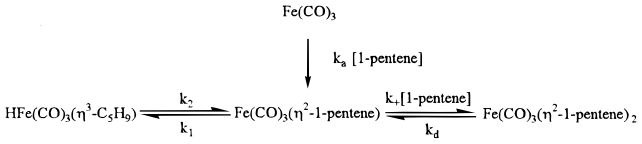

When $Fe(CO)_3$ reacts with ethylene in the gas phase, the unsaturated mono-ethylene adduct, $Fe(CO)_3(\eta^2\text{-}C_2H_4)$, is produced with a bimolecular rate constant of $(2.2 \pm 0.2) \times 10^{-10}$ cm^3 molecule^{-1} s^{-1},[40] within a factor of 2 of the rate constant for reaction of $Fe(CO)_3$ with 1-pentene. The formation of a monoolefin adduct as the initial product is a recurring theme in the reaction of coordinatively unsaturated metal carbonyls and olefins.[41] Matrix isolation studies also support the initial formation of a monoolefin complex and show the π-allyl metal hydride to be more thermodynamically stable.[14] These observations suggest a mechanism for the formation of $HFe(CO)_3(\eta^3\text{-}C_5H_9)$ that is an analogue of the mechanism that has been proposed for propene.[16]

Thus, as with the $Fe(CO)_3$/propene system, the lack of observation of $Fe(CO)_3(\eta^2$-1-pentene) in the gas phase, at 296 K, results from rapid β-hydrogen transfer that follows the rate-limiting addition of 1-pentene to $Fe(CO)_3$ (Scheme 2). Therefore, the initial steps in the $Fe(CO)_5$/1-pentene system exhibit the characteristic behavior of an A $\rightarrow$ B $\rightarrow$ C process where A = $Fe(CO)_3$, B = $Fe(CO)_3$(olefin), and C = $HFe(CO)_3(\pi$-allyl), with a sufficiently fast B $\rightarrow$ C step that the intermediate B is not observed.[38] These reactions are shown in Scheme 2 with rate constants k_a and k_1, respectively. B is not observable even after an equilibrium is established since it has a very small equilibrium concentration (vida infra).

Though the monoolefin and bisolefin adducts in Scheme 2 are identified as η^2-complexes of 1-pentene, as the monoolefin complex comes into equilibrium with $HFe(CO)_3(\eta^3\text{-}C_5H_9)$, isomerization of 1-pentene can occur. This will be discussed in more detail in Section IV.B.2. Due to the possibility of isomerization, from this point on, the mono- and bisolefin complexes will be referred to "generically" as $Fe(CO)_3$(pentene) and $Fe(CO)_3$(pentene)$_2$.

B. Millisecond Time Scale: Formation of Species II. 1. Assignment. $HFe(CO)_3(C_5H_9)$ decays on the millisecond time scale with concurrent formation of species II at 1985 cm^{-1}. Reference to Table 1 reveals that in neat 1-pentene at 195 K, $Fe(CO)_3$(1-pentene)$_2$ absorbs at 2048 and 1972 cm^{-1}. The 13 cm^{-1} gas to condensed phase red shift of the lower frequency band is once again of a typical magnitude for a gas phase relative to the corresponding matrix absorption.[39] Table 1 also shows that the absorption bands of $Fe(CO)_3(C_3H_6)_2$ occur at 2060 and 1988 cm^{-1} in the gas phase, the latter of which is virtually identical with that for species II. The higher frequency band of $Fe(CO)_3$(olefin)$_2$ is considerably weaker than the lower frequency band, being in the ratio of 1:11 and 1:16.6 in hydrocarbon glasses for olefin = propene and 1-pentene, respectively.[42] Due to its much smaller absorbance, the higher frequency absorption of $Fe(CO)_3(C_3H_6)_2$ was not readily apparent in a time-resolved spectrum but was evident in individual traces taken at 2060 cm^{-1}.[16] The analogous higher frequency band of $Fe(CO)_3$(pentene)$_2$ was not observed in these gas-phase studies, presumably due to a lower signal-to-noise ratio. In light of the correspondence with matrix absorptions and the similarity in behavior of this species with the analogous species in the propene system, species II is assigned as the bispentene adduct, $Fe(CO)_3$(pentene)$_2$. As alluded to above and discussed in more detail in the next section, this bispentene adduct may be either a bis-1-pentene species or a mixed bispentene adduct.

2. Mechanism. On a millisecond time scale, $HFe(CO)_3(\eta^3\text{-}C_5H_9)$ decays and formation of $Fe(CO)_3(\eta^2$-pentene)$_2$ is observed. This behavior is consistent with the kinetics shown in Scheme 2 in which $Fe(CO)_3(\eta^2$-pentene) is shown in equilibrium with *both* $HFe(CO)_3(\eta^3\text{-}C_5H_9)$ and $Fe(CO)_3(\eta^2$-pentene)$_2$. The potentially more direct pathway, which could lead to formation of $Fe(CO)_3(\eta^2$-pentene)$_2$ and involves stepwise addition of two 1-pentene ligands to $Fe(CO)_3$, does not occur initially because at the experimentally accessible pressures of 1-pentene, the addition of the second 1-pentene ligand cannot compete with rapid β-hydrogen transfer, i.e., k_1 is sufficiently larger than k_+[1-pentene]. Analogous behavior was observed in the $Fe(CO)_5$/C_3H_6 system.[16]

As a consequence of this rapid β-hydrogen transfer the rate constant for the addition of C_3H_6 to $Fe(CO)_3(C_3H_6)$ cannot be directly measured. However, it can be estimated. This was done in the propene system by determining the rate constant for addition of C_2H_4 and C_3H_6 to $Fe(CO)_3(C_2H_4)$. Monitoring this addition step was possible because C_2H_4 does not have β-hydrogens and thus β-hydrogen transfer cannot occur for the $Fe(CO)_3(C_2H_4)$ adduct.[16] Instead, ethylene undergoes stepwise olefin addition to form $Fe(CO)_3(C_2H_4)$ and $Fe(CO)_3(C_2H_4)_2$ after UV photolysis of $Fe(CO)_5$ in the presence of C_2H_4.[40] Similarly, the rate of propene addition to $Fe(CO)_3(C_2H_4)$ can be measured. These same measurements[16] can be used to provide an estimate

(40) Hayes, D. M.; Weitz, E. *J. Phys. Chem.* **1991**, *95*, 2723.

(41) (a) Hill, C. L., Ed. *Activation and Functionalization of Alkanes*; Wiley: New York, 1989. (b) Parshall, G. W. *Homogeneous Catalysis*; Wiley: New York, 1980; Chapter 7.

(42) Wuu, Y.; Bentsen, J. G.; Brinkley, C. G.; Wrighton, M. S. *Inorg. Chem.* **1987**, *26*, 530.

for the rate constant for the addition of 1-pentene to $Fe(CO)_3$(pentene) of $k_+ = 1.6 \times 10^{-11}$ cm^3 molecule^{-1} s^{-1}.

For the $Fe(CO)_5$/1-pentene system, the fact that initially no $Fe(CO)_3$(1-pentene)$_2$ and only $HFe(CO)_3(C_5H_9)$ is observed, following the reaction of $Fe(CO)_3$ and 1-pentene, up to readily accessible pressures of 1-pentene (~400 Torr) is compatible with $k_1 \gg k_+$[1-pentene] in Scheme 2, as was observed in the propene system. This behavior can also be used to estimate a lower limit for k_1. Computing k_+[1-pentene] at 400 Torr and taking into account that the *initial formation* of 20% of the final amount of the bispentene adduct could be readily observed leads to an estimation of a lower bound for k_1 of $\sim 10^9$ s^{-1}.

The distribution of photoproducts in a given system can have a pressure dependence.[29,30] Though we have no direct evidence for a shift in product distribution as a function of olefin pressure, it is possible, at least in principle, that for 308-nm photolysis, at the highest pressure of 1-pentene (400 Torr), which has allowed us to establish the lower bounds for β-hydrogen transfer, the product distribution shifts to produce primarily or exclusively $Fe(CO)_4$. If this were to happen then the initially formed reaction product would be $Fe(CO)_4$(1-pentene). Since the rate of formation of the bisolefin species was measured in a static cell, photolysis of $Fe(CO)_4$(1-pentene) by subsequent laser pulses could produce $Fe(CO)_3$(1- pentene). However, there would then still be a competition between β-hydrogen transfer and formation of the bisolefin species that would effectively be identical with the competition that occurs after $Fe(CO)_3$ adds 1-pentene. Thus, even in this case, the lack of observation of a significant quantity of initially formed bisolefin species can be taken as evidence that $k_1 \geq 10^9$ s^{-1} for 1-pentene. In Scheme 2 the initially formed unsaturated 16-e$^-$ $Fe(CO)_3(\eta^2$-1-pentene) adduct will form a saturated 18-e$^-$ species either by β-hydrogen transfer to give $HFe(CO)_3(\eta^3$-$C_5H_9)$ or by the bimolecular addition of 1-pentene, which generates $Fe(CO)_3(\eta^2$-1-pentene$)_2$. However, once $HFe(CO)_3(\eta^3$-$C_5H_9)$ is formed by rapid β-hydrogen transfer, formation of $Fe(CO)_3(\eta^2$-1-pentene$)_2$ is much slower than would be anticipated based simply on the magnitude of the rate constant, k_+. There is also the question of why the rate of formation of the bisolefin complex is *independent* of 1-pentene pressure. Both the slow rate of formation of $Fe(CO)_3(\eta^2$-1-pentene$)_2$ and its pressure independence can be understood based on the kinetics of the system.

3. Kinetics. The behavior of the 1-pentene system as well as the propene system[16] is consistent with the mechanism shown in Scheme 1 and delineated in eqs 1−4 below.

$$Fe(CO)_5 + h\nu \xrightarrow{308\ nm} Fe(CO)_3 + 2CO \quad (1)$$

$$Fe(CO)_3 + olefin \xrightarrow{k_a} Fe(CO)_3(\eta^2\text{-olefin}) \quad (2)$$

$$Fe(CO)_3(\eta^2\text{-olefin}) \underset{k_2}{\overset{k_1}{\rightleftharpoons}} HFe(CO)_3(\eta^3\text{-allyl}) \quad (3)$$

$$Fe(CO)_3(\eta^2\text{-olefin}) + olefin \underset{k_d}{\overset{k_+}{\rightleftharpoons}} Fe(CO)_3(\eta^2\text{-olefin})_2 \quad (4)$$

Taking $Fe(CO)_3(\eta^2$-pentene) as a steady-state intermediate, with appropriate simplifications (namely: (1) k_+[olefin] $\gg k_d$ and (2) $k_1 \gg k_2$), and inclusion of mass conservation the following expression for the rate of change of the bisolefin species, which is indicated as dB/dt, can be derived:

$$dB/dt = \frac{-B[k_1k_d + k_2k_+[olefin]] + k_2k_+[olefin]A_0}{k_1 + k_+[olefin]} \quad (5)$$

In this expression A_0 is the sum of the concentrations of the π-allyl hydride, the monoolefin, and the bisolefin (B) complexes. Both inequalities hold for the propene system and the first inequality holds, at experimentally relevant pressures, for a variety of bisolefin species.[28,47] As will be shown in the subsequent development, these inequalities hold for 1-pentene.

Rearranging the expression in eq 5 gives:

$$\int \frac{dB}{\frac{-B[k_1k_d + k_2k_+[olefin]]}{k_1 + k_+[olefin]} + \frac{k_2k_+[olefin]A_0}{k_1 + k_+[olefin]}} = \int dt \quad (6)$$

The left-hand side of this equation has the form

$$\int dB/(aB + b), \text{ which is equal to } 1/a(\ln(aB + b)) \quad (7)$$

where

$$a = -\frac{[k_1k_d + k_2k_+[olefin]]}{k_1 + k_+[olefin]} \quad (8)$$

and

$$b = \frac{k_2k_+[olefin]A_0}{k_1 + k_+[olefin]} \quad (9)$$

provided the argument of the ln term in eq 7 is positive. Since the first term in the denominator of eq 6 is negative, this condition is equivalent to $b > -aB$. Since B is a maximum at equilibrium, if $b > -aB$ at equilibrium, then the solution to eq 7 is valid for all conditions for this system.

From mass conservation and the relationship between the relevant rate constants and the equilibrium concentrations of the species in this system the following expression can be derived.

$$\frac{A_0}{B_{eq}} = 1 + \frac{k_dk_1}{k_2k_+[olefin]} + \frac{k_d}{k_+[olefin]} \quad (10)$$

Solving for A_0 using eq 10 and substituting in eq 9 and simplifying reduces the inequality that must be satisfied to:

$$-k_2k_d < 0 \quad (11)$$

Thus, it is clear the inequality, $b > -aB$ must hold since k_2k_d is a positive quantity. Therefore, eq 6 can be integrated as indicated and the resulting expression obtained for $B(t)$ is:

$$B(t) = \frac{b}{a}(e^{at} - 1) \quad (12)$$

In this expression $-a$ is the observed rate of formation of the bisolefin species which we designate as k_{obs}. The exact form of the expression for $B(t)$ can be obtained by substituting in a and b from eqs 8 and 9. However, the expression for a in eq 12, and thus k_{obs}, can be further simplified by applying the inequality

(43) Seder, T. A.; Ouderkirk, A. J.; Weitz, E. *J. Chem. Phys.* **1986**, *85*, 1977.

(44) (a) Long, G. T. Unpublished results. (b) Long, G. T. Ph.D. Thesis, Northwestern University, 1998.

(45) Holbrook, K. A.; Pilling, M. J.; Robinson, P. J. *Unimolecular Reactions*, 2nd ed.; Wiley-Interscience: London, 1997.

(46) McMillen, D. F.; Golden, D. M. *Annu. Rev. Phys. Chem.* **1982**, *33*, 493.

(47) House, P. G.; Weitz, E. *Chem. Phys. Lett.* **1997**, *266*, 239.

$k_1 \gg k_+$[olefin] to give:

$$-a = k_{obs} = K_{eq}k_+[\text{olefin}] + k_d \quad (13)$$

Recall that the inequality $k_1 \gg k_+$[olefin] was established based on the absence of any observable *initial* (prompt) formation of a bispentene complex.

Interestingly, there are two limiting cases for the expression in eq 13 depending on the relative magnitudes of the two terms, $K_{eq}k_+$[olefin] and k_d. For a given value of K_{eq} and k_+, when the olefin pressure is such that k_d is sufficiently larger than $K_{eq}k_+$[olefin] that this latter pressure-dependent term makes a negligible contribution to k_{obs}, k_{obs} will be independent of olefin pressure. This can account for the effectively pressure-independent rise rate of the absorption due to the bisolefin complex that is observed for 1-pentene over the experimentally accessible pressure range. Under these circumstances k_d can be directly determined (i.e., $k_d \approx k_{obs}$) and, with a knowledge of k_+, an upper limit on K_{eq} can be established based on the fact that k_d must sufficiently exceed k_+K_{eq}[olefin] that k_{obs} reduces to k_d within experimental error. Given the estimated value of k_+ of 6×10^5 Torr^{-1} s^{-1}, and the readily available maximum pressure of 400 Torr for 1-pentene, K_{eq} must be on the order of $\sim 2 \times 10^{-8}$ or less to give, within experimental error, the observed pressure independence for the rate of formation of the bispentene complex. The value of k_{obs} is then approximately k_d, which for this system is 20 s^{-1} at 296 K, and the activation energy for this process is 19.6 $\pm$ 0.7 kcal/mol. A computer model of the kinetics, based on numerical integration of eqs 1−4, provided additional verification that K_{eq} must be on the order of 10^{-8} to give a pressure-independent rate for the rise of species II and, given reasonable values for the expected error on k_{obs}, when this occurs, $k_{obs} \approx k_d$. The pressure independence of the rate of rise of species II further validates the inequality, $k_1 \gg k_2$.

If k_d does not exceed $K_{eq}k_+$[olefin] by a suitable amount, then K_{eq} can be directly determined from the pressure dependence of k_{obs} using the estimated value for k_+. For propene, K_{eq} was determined to be 2.4×10^{-5}.[16] Since k_d has been estimated as 10 s^{-1} for Fe(CO)$_3$(C$_3$H$_6$)$_2$ and k_+ as 6×10^5 s^{-1} Torr^{-1}, it is clear that k_d can be neglected relative to $K_{eq}k_+$[propene] even at a pressure as low as ~10 Torr. Under these circumstances, eq 13 will reduce to $k_{obs} = K_{eq}k_+$[propene]. From this comparison is it clear that it is possible to neglect the dissociation of Fe(CO)$_3$(propene)$_2$ in eq 4 at the pressures at which formation of the bispropene species was monitored. Neglect of the dissociation of the bisolefin adduct in eq 4 leads to a more direct derivation of k_{obs} as $K_{eq}k_+$[propene] via the steady-state approximation. This approach was taken in ref 16.

It is interesting to note that eq 13 is analogous to what would be expected for the approach to equilibrium for a reversible first-order (or in this case, first-order in one direction and pseudo-first-order in the other direction) reaction. This of course implies that the decay of the π-allyl hydride and the rise of the monoolefin species should be the same since one is decaying to form the other. Figure 5 shows a typical transient waveform taken at 2067 cm^{-1}, characteristic of the π-allyl hydride. In the inset to this figure this signal has been inverted and the data have been scaled to facilitate a visual comparison with a transient waveform taken under comparable conditions at 1984 cm^{-1}. The agreement in rates that was anticipated is apparent from visual inspection. Since the monoolefin adduct and the π-allyl hydride reach equilibrium, with the π-allyl hydride being present in much higher concentration than the monoolefin species, well before they equilibrate with the bisolefin complex, the forward rate constant for the approach to the subsequent equilibrium is weighted by K_{eq}. Thus a shift in K_{eq} by a suitable amount can lead to either a *pressure-dependent or a pressure-independent* rise of the bisolefin species in such a system.

The extent of the decay of the transient waveforms of HFe(CO)$_3$(η^3-C$_5$H$_9$) can be used as another means of determining a value for K_{eq}. The traces at 2067 cm^{-1}, such as the one shown in Figure 5, decay to ~60−80% of their initial amplitude when ~400 Torr of 1-pentene is present. This amplitude change can be related to the equilibrium ratio of Fe(CO)$_3$(η^2-pentene)$_2$ to HFe(CO)$_3$(η^3-C$_5$H$_9$) (see Scheme 2) as shown in the following equation where the percent (%) refers to the remaining percentage of HFe(CO)$_3$(η^3-C$_5$H$_9$) after an equilibrium is established between HFe(CO)$_3$(η^3-C$_5$H$_9$) and Fe(CO)$_3$(η^2-pentene)$_2$.

$$\frac{[\text{Fe(CO)}_3(\eta^2\text{-pentene})_2]}{[\text{HFe(CO)}_3(\eta^3\text{-C}_5\text{H}_9)]} = \frac{1 - \%}{\%} \quad (14)$$

The equilibrium ratio of Fe(CO)$_3$(η^2-pentene)$_2$ to HFe(CO)$_3$(η^3-C$_5$H$_9$) can be expressed as the ratio of the equilibrium constants for the equilibria in Scheme 2. Thus the right-hand side of eq 14 is equal to:

$$\frac{k_2k_+(\text{olefin})}{k_1k_d} \quad (15)$$

and

$$K_{eq} = \frac{\frac{(1 - \%)}{\%}k_d}{k_+(\text{olefin})} \quad (16)$$

Using a value of $k_+ = 1.6 \times 10^{-11}$ cm^3 molecule^{-1} s^{-1}, as discussed above, and the measured value of $k_d = 20$ s^{-1}, if % = 60, $K_{eq} = \sim 6 \times 10^{-8}$ and a value of % = 80 gives $K_{eq} \sim 2 \times 10^{-8}$. The range of $K_{eq} \sim 2 \times 10^{-8}$ to 6×10^{-8} determined from amplitude data is similar to the value of $K_{eq} \leq 2 \times 10^{-8}$ determined from rate data (vide supra) and from this comparison $\sim 2 \times 10^{-8}$ is taken as the value of K_{eq} to be used in subsequent calculations. However, clearly this value for K_{eq} has significant uncertainty associated with it.

It is interesting to note that the back β-hydrogen transfer from HFe(CO)$_3$(η^3-C$_5$H$_9$) in Scheme 2 may be either to the C3 carbon to regenerate Fe(CO)$_3$(η^2-1-pentene) or to the C1 carbon, which gives rise to an isomerized monoolefin adduct, Fe(CO)$_3$(η^2-2-pentene). For the latter case, subsequent addition of 1-pentene to Fe(CO)$_3$(η^2-2-pentene) generates a mixed bisolefin adduct, Fe(CO)$_3$(η^2-1-pentene)(η^2-2-pentene). It is questionable whether the infrared absorptions of Fe(CO)$_3$(η^2-1-pentene)$_2$ and Fe(CO)$_3$(η^2-1-pentene)(η^2-2-pentene), in the CO stretching region, are sufficiently different to render them distinguishable by time-resolved IR spectroscopy. If Fe(CO)$_3$(η^2-1-pentene)(η^2-2-pentene) does form, and the material discussed in this section suggests it does, the measured value of k_d and its temperature dependence would then reflect a weighted average for the loss of 1-pentene and 2-pentene from Fe(CO)$_3$(η^2-pentene)$_2$. The Arrhenius plot of Figure 6 gives an activation energy of E_a = 19.6 $\pm$ 0.7 kcal mol^{-1} and a preexponential factor of $A = 5.3 \times 10^{15}$ s^{-1} for this process. The similarity of this value to those for the loss of olefin from Fe(CO)$_3$(olefin)$_2$ for olefin = propene, $E_a \sim 19$ kcal mol^{-1},[16] and for olefin = ethylene, $E_a = 21.7$ kcal mol^{-1},[28a] both of which occur by a dissociative mechanism, suggests that the loss of pentene from Fe(CO)$_3$(pentene)$_2$ or Fe(CO)$_3$(pentene)(pentene′) proceeds by a similar mechanism.

4. Thermochemistry. Thermochemical information can be determined from the equilibrium constant for the equilibrium between $HFe(CO)_3(\eta^3\text{-}C_5H_9)$ and $Fe(CO)_3(\eta^2\text{-pentene})$ using the standard relation

$$\Delta G = -RT \ln K_{eq} \quad (17)$$

At the standard ambient temperature of 298 K and a pressure of 1 bar (SATP), ΔG is calculated to be $\sim$10.5 kcal mol^{-1} for the process, $HFe(CO)_3(\eta^3\text{-}C_5H_9) \rightarrow Fe(CO)_3(\eta^2\text{-pentene})$. The uncertainties in K_{eq} should be taken into account in the interpretation of ΔG and other thermodynamic parameters derived from K_{eq}.

Though the two additional methylene groups in both $HFe(CO)_3(C_5H_9)$ and $Fe(CO)_3$(pentene) would be expected to affect the absolute entropy of each species, it seems plausible that they would not have a significant effect on the *entropy difference* between the π-allyl hydride and the monoolefin complexes, in the respective systems, since the bond-breaking and bond-making steps in these reactions do not involve the additional methylene groups. Thus, it seems reasonable to assume that the entropic contributions to the free energy are similar for this conversion in the pentene system to what has been determined for the analogous process for propene. With this assumption, a ΔS of 3 ± 2 cal K^{-1} mol^{-1}, as determined for the propene system[16] for the processes $HFe(CO)_3(\eta^3\text{-}C_3H_5) \rightarrow Fe(CO)_3(\eta^2\text{-}C_3H_6)$, can be used to calculate a ΔH of $\sim$11.4 kcal mol^{-1} for the process $HFe(CO)_3(\eta^3\text{-}C_5H_9) \rightarrow Fe(CO)_3(\eta^2\text{-pentene})$ at SATP.

Thermochemical parameters can also be determined for the equilibrium between $Fe(CO)_3(\eta^2\text{-1-pentene})$ and $Fe(CO)_3(\eta^2\text{-pentene})_2$ (Scheme 2) and yield $\Delta G \sim -9.9$ kcal mol^{-1} for the process $Fe(CO)_3(\eta^2\text{-pentene}) \rightarrow Fe(CO)_3(\eta^2\text{-pentene})_2$ at SATP based on a value for K'_{eq} (where the prime is used to distinguish the equilibrium constant for this equation from K_{eq} used for the π-allyl hydride monoolefin equilibrium) calculated from reported data. The resulting bond enthalpy, $\Delta H = 20.2 + 0.7$ kcal mol^{-1}, may reflect a weighted average for loss of 1-pentene and 2-pentene (vide supra). ΔS for the same process can be calculated to be ca. -35 cal K^{-1} mol^{-1} at 298 K. These parameters show that the enthalpy serves as the thermodynamic driving force for the formation of $Fe(CO)_3(\eta^2\text{-pentene})_2$, as ΔH exceeds the product of the temperature times the entropy lost in formation of this complex. Since there are estimates inherent in the determination of K'_{eq}, most notably the exact value of k_+, the values of the thermodynamic parameters derived from K'_{eq} should be regarded as estimates, albeit ones that are likely to be very good.

C. Long Time Scale Formation of Species III. 1. Assignment. Species III, with infrared absorption bands at 2089 and 1995 cm^{-1}, is observed by time-resolved FTIR spectroscopy following 355-nm photolysis of a mixture of $Fe(CO)_5$, 1-pentene, and helium (see Figure 7). Table 1 shows that these absorption bands are consistent with the highest and lowest frequency absorptions of $Fe(CO)_4$(1-pentene) in 3-methylpentane at 298 K, which absorbs at 2083, 2002, and 1981 cm^{-1}. The middle absorption band of $Fe(CO)_4$(1-pentene), anticipated to be at $\sim$2012 cm^{-1} in the gas phase, is probably obscured by the overlapping absorption of $Fe(CO)_5$ centered at 2014 cm^{-1}. Also, the low-frequency band probably peaks a few cm^{-1} higher than the observed peak since its high-frequency edge is truncated by the $Fe(CO)_5$ absorption (Figure 7). In the analogous propene system the gas-phase bands of $Fe(CO)_4(C_3H_6)$ were at 2089, 2014, and 1988 cm^{-1} (Table 1). The correspondence between the observed IR absorptions and those reported for $Fe(CO)_4$(olefin) complexes in the gas phase and other media are consistent with species III being $Fe(CO)_4$(1-pentene). However, it is not clear whether an $Fe(CO)_4$(pentene) complex involving another pentene isomer could be distinguished, via its IR absorptions in the CO stretching region, from $Fe(CO)_4$(1-pentene). An enhancement in the quantity of species III produced when CO is added to the photolysis cell is also consistent with the assignment of species III as $Fe(CO)_4$(pentene).

2. Mechanism. $Fe(CO)_4$(pentene) can form by a number of pathways. Based on the product distribution measured after 351-nm photolysis[43] and the expected trend for the energy dependence of the yield of photoproducts,[29] the 355-nm output of a frequency tripled Nd:YAG laser, used as the photolysis source in time-resolved FTIR experiments, is expected to generate both $Fe(CO)_4$ and $Fe(CO)_3$ as primary photoproducts. The most direct pathway for formation of $Fe(CO)_4$(1-pentene) involves addition of 1-pentene to photolytically generated $Fe(CO)_4$. Other pathways involving secondary photolysis and/or addition of photolytically generated CO (or added CO) to an unsaturated $Fe(CO)_3$(olefin) adduct are also possible.[37,44b] For example, $Fe(CO)_4$(pentene) can form via an $Fe(CO)_3$(pentene) complex which contains an isomerized olefin. Thus, in principle, the $Fe(CO)_4$(pentene) complex generated in this study could also involve a mixture of pentene isomers. It should be noted that though formation of $Fe(CO)_4$(pentene) can terminate a thermal catalytic cycle, photolysis of $Fe(CO)_4$(pentene) by the next laser pulse, which can lead to formation of $Fe(CO)_3$(pentene), allows this species to reenter the catalytic cycle.

It should also be noted that even though $Fe(CO)_4$(pentene) is formed on the time scale of the collection of FTIR data, under experimental conditions, this species is not evident on the time scale of formation of $HFe(CO)_3(\eta^3\text{-}C_5H_9)$ or $Fe(CO)_3(pentene)_2$. Photolysis using 308-nm radiation was employed in studies of the rates of formation and generation of transient spectra of species I and II. The lack of evidence for formation of $Fe(CO)_4$(pentene) on the time scale for formation of $HFe(CO)_3(\eta^3\text{-}C_5H_9)$ or $Fe(CO)_3(pentene)_2$ is consistent with $Fe(CO)_3$ being the only coordinatively unsaturated product produced in significant yield using 308 nm photolysis radiation, even at a few hundred Torr of total pressure. Under these conditions $Fe(CO)_4$(pentene) would have to form by addition of CO to $Fe(CO)_3$, with subsequent addition of pentene, or via addition of CO to an $Fe(CO)_3$(pentene) intermediate. For either pathway the addition of CO to these two intermediate species must compete with addition of 1-pentene. In the absence of added CO, the only source of CO is from photolysis of $Fe(CO)_5$. The kinetics of addition of 1-pentene to $Fe(CO)_3$(pentene) were studied in a static cell at a minimum pentene pressure of 50 Torr. Thus, even assuming complete photolysis of all $Fe(CO)_5$ in the cell, which would generate 2 CO molecules per $Fe(CO)_5$ molecule, the 1-pentene-to-CO ratio would be at least 250:1. Though the rate of addition of CO to $Fe(CO)_3$(pentene) is not known, this rate can be estimated using a procedure similar to that used to estimate the rate of addition of 1-pentene to $Fe(CO)_3$(pentene). Based on the ethylene system the ratio of rates for addition of olefin versus CO to $Fe(CO)_3$(olefin) is $\sim$2.[47] Thus, negligible $Fe(CO)_4$(pentene) would form via this pathway. The formation of $Fe(CO)_3$(1-pentene) as a result of addition of 1-pentene to $Fe(CO)_3$ was studied in a flow cell in the absence of added CO. Since the flow rate was set such that the cell empties between laser pulses the only CO present is produced as a result of ca. one photolysis pulse. Since this addition process was studied at a much lower pressure of 1-pentene, the data in Figure

1 provide relevant evidence that formation of $Fe(CO)_4$ is expected to be negligible. Similarly, formation of $Fe(CO)_4$-(pentene) under these conditions is expected to be negligible.

However, in a static cell, on the much longer time scales involved in the collection of FTIR data, the bisolefin species has the potential to undergo multiple cycles of olefin loss. $Fe(CO)_4$(pentene) could form, via CO addition, at some point during these cycles. As depicted in Scheme 4 in Section V, each time an olefin is lost CO has the opportunity to add to $Fe(CO)_3$(pentene) to form a species that is stable on the relevant time scale for observation and is thus at least temporarily removed from the reaction cycle (it can be reintroduced by photolysis). Additionally, the FTIR experiments were conducted using 355-nm radiation which produces $Fe(CO)_4$ as well as $Fe(CO)_3$. As indicated in the discussion above, addition of 1-pentene to $Fe(CO)_4$ provides a direct route to formation of $Fe(CO)_4$(pentene). However, we have no evidence that $Fe(CO)_4$ is produced in significant quantities with 308-nm photolysis under experimental conditions. Thus, the lack of direct photolytic production of $Fe(CO)_4$ would preclude a significant role for this potentially direct pathway to $Fe(CO)_4$(pentene).

Permanent loss pathways for iron-containing species are also possible. $Fe(CO)_5$ can react with unsaturated species such as $Fe(CO)_3$(pentene) or $Fe(CO)_4$ to form polynuclear complexes.[37] Formation of such complexes can occur with rate constants that approach the gas kinetic limit.[37] However, in the presence of a large excess of 1-pentene, the formation of binuclear iron complexes is unlikely to be important in the kinetics of an individual catalytic cycle. None of the data from this study suggest a significant role for a reaction of parent with any unsaturated species in a given catalytic cycle. Such reactions would be expected to make only a minor contribution to any subsequent kinetics as these types of binuclear iron complexes are usually nonvolatile. Nevertheless, formation of polynuclear iron complexes would be anticipated to contribute as a permanent loss pathway in the catalytic turnover cycle since in each reaction step it is possible to form polynuclear iron species.

D. Comparison with the $Fe(CO)_5$/Propene System. The qualitative mechanism for olefin isomerization in the $Fe(CO)_5$/propene and $Fe(CO)_5$/1-pentene systems is identical (see eqs 1−4). For readily accessible pressures of both propene and 1-pentene, β-hydrogen transfer in the $Fe(CO)_3(\eta^2$-olefin) complex is faster than the immediate addition of another olefin to $Fe(CO)_3(\eta^2$-olefin). For propene, it is possible to set a somewhat higher lower bound for the rate of β-hydrogen transfer (k_1) due to the fact that the vapor pressure of propene, at or near room temperature, is higher than that for 1-pentene. Thus, the reported differences in the lower limits of the rate of β-hydrogen transfer in the two systems may result from this factor rather than any intrinsic difference in the actual kinetics of β-hydrogen transfer in the systems.

Though the propene and 1-pentene systems can be described by the same set of kinetic equations (1−4) the ∼3 orders of magnitude shift in equilibrium constant for the equilibrium between $HFe(CO)_3(\pi$-allyl) and $Fe(CO)_3$(olefin) (toward the π-allyl metal hydride) for olefin = 1-pentene relative to propene leads to different observations for the kinetics of these systems, particularly for the formation of the bisolefin species. As discussed in Section IV.B.3, this shift alters the form of the observed rate of formation of $Fe(CO)_3(olefin)_2$, being dependent on olefin pressure in the $Fe(CO)_5$/propene system and independent of olefin pressure in the $Fe(CO)_5$/1-pentene system.

The difference in the BDEs for the β-hydrogens of propene and 1-pentene may have important ramifications in iron carbonyl-catalyzed olefin isomerization. The BDE for the β-hydrogen in propene has been measured to be 86 ± 2 kcal mol^{-1}.[46] Although to our knowledge the BDE for the β-hydrogens in 1-pentene has not been measured, the analogous β-hydrogen BDE in 1-butene has been determined to be 82 ± 1 kcal mol^{-1}.[46] The ∼4 kcal mol^{-1} smaller BDE for the C3−H bond relative to the C1−H bond suggests that back β-hydrogen transfer to the C1 carbon in $HFe(CO)_3(\eta^3$-$C_5H_9)$ should form $Fe(CO)_3(\eta^2$- 2-pentene) preferentially. If $Fe(CO)_3(\eta^2$- 2-pentene) does form preferentially, the presence of excess 1-pentene in the current study would lead to the formation of a mixed bisolefin adduct, $Fe(CO)_3(\eta^2$- 1-pentene)(η^2- 2-pentene), upon the addition of 1-pentene to $Fe(CO)_3(\eta^2$- 2-pentene). As indicated in Section IV.B.4, if $Fe(CO)_3(\eta^2$-1-pentene)(η^2-2-pentene) does form, the measurement of the unimolecular rate constant for loss of pentene from $Fe(CO)_3(pentene)_2$, k_d, will correspond to a weighted average for the loss of 1-pentene and 2-pentene.

E. Thermochemistry. As indicated in Section IV.B.4, the equilibrium constant, $K'_{eq} = k_+$[1-pentene]/k_d, for the equilibrium between $Fe(CO)_3(\eta^2$-olefin) and $Fe(CO)_3(\eta^2$-olefin)$_2$ can be used to determine thermochemical information. Since the same value of k_+ was used as an estimate for the rate constant for the addition of olefin to $Fe(CO)_3$(olefin) for both propene and 1-pentene, the difference in the K'_{eq} for the two systems lies in the rate constant for unimolecular dissociation of olefin from $Fe(CO)_3(olefin)_2$, k_d, which has a value of 20 s^{-1} for 1-pentene and 10 s^{-1} for propene.[16] From these values of k_d, $K'_{eq} \sim 4 \times 10^7$ and $\sim 2 \times 10^7$ bar^{-1} for propene and pentene, respectively, at 296 K. Substituting these values into eq 5 yields free energies of $\Delta G \sim -10.3$ and -9.9 kcal mol^{-1} for propene and 1-pentene, respectively, at SATP for the process $Fe(CO)_3$-(olefin) → $Fe(CO)_3(olefin)_2$. Given the uncertainties in the value for K_{eq} for the 1-pentene system and in k_+ for both systems, these differences should not be considered as significant. The bond enthalpy for the loss of olefin from $Fe(CO)_3(olefin)_2$ has been estimated as ∼19 kcal mol^{-1} for olefin = propene. The value for pentene, though it is likely to involve both a bis-1-pentene and a mixed bispentene species, can be computed from measured experimental data as 20.2 ± 0.6 kcal mol^{-1}. Using these values leads to $\Delta S \sim -29$ and -35 cal K^{-1} mol^{-1} at SATP for olefin = propene and pentene, respectively. Though there are uncertainties involved in the calculation of these parameters, they clearly indicate a large change in entropy on association of a second olefin to form an $Fe(CO)_3(olefin)_2$ complex. This large change in entropy can be verified by another approach.

The overall entropies for ligand addition can also be calculated from the difference of the entropies of activation for ligand addition and for unimolecular loss of ligand using activated complex theory. As the process in (18) is the reverse

$$M(CO)_xL_{y-1} + L \xrightarrow{k_+} M(CO)_xL_y \qquad (18)$$

of that in (19), by microscopic reversibility these processes

$$M(CO)_xL_y \xrightarrow{k_d} M(CO)_xL_{y-1} + L \qquad (19)$$

proceed through a common transition state.[38] Thus, it is possible to determine how these processes contribute to the overall entropy change. The overall entropy change for the process shown in (18) can then be computed from the magnitudes of the activation entropies for (18) and (19) (Scheme 3). This scheme and Table 2, which contains tabulated values of the entropies of activation for the processes in (18) and (19), show

Table 2. Overall Entropies for the Reactions $Fe(CO)_3L + L \rightarrow Fe(CO)_3L_2$ and $Cr(CO)_5 + C_2H_4 \rightarrow Cr(CO)_5(C_2H_4)$

$M(CO)_x$ or $M(CO)_xL$	L	T (K)	$10^{11}\cdot k_+$ (cm^3 $molec^{-1}$ s^{-1})	$\Delta S^{\ddagger}(18)$ (cal K^{-1} mol^{-1})	k_d (s^{-1})	ln A	$\Delta S^{\ddagger}(19)$ (cal K^{-1} mol^{-1})	ΔS (cal K^{-1} mol^{-1})
$Fe(CO)_3(C_2H_4)$[a]	C_2H_4	297	1.1 ± 0.8	$-23._9$	0.15	33 ± 3	$5._1$	-29
$Fe(CO)_3(C_3H_6)$[b]	C_3H_6	296	~ 1.5	$-23._3$	10	33	$5._1$	-28
$Fe(CO)_3$(pentene)[c]	1-C_5H_{10}	296	~ 1.5	$-23._3$	20	36	$11._4$	-35
$Cr(CO)_5$[d]	C_2H_4	303	19 ± 2[e]	$-18._4$	0.17	38	$15._4$	-34

[a] Reference 28a. [b] Reference 16. [c] This work. [d] Reference 48b. [e] Reference 28b.

Scheme 3

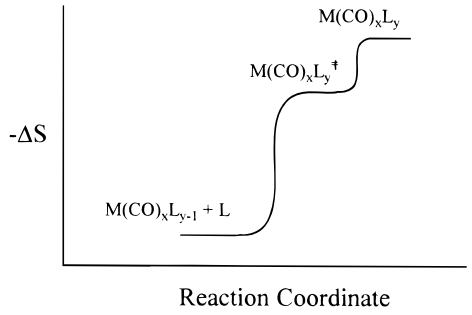

that the addition of ligand to $M(CO)_xL_{y-1}$ to form the transition state, $M(CO)_xL_y^{\ddagger}$, has a larger contribution to the overall entropy than that for the shortening of the M−L bond in going from the transition state $M(CO)_xL_y^{\ddagger}$ to $M(CO)_xL_y$. For the $Fe(CO)_5$ system, the addition of CO to $Fe(CO)_4$ to form $Fe(CO)_5$ is a spin-forbidden reaction since $Fe(CO)_4$ has a triplet ground state and $Fe(CO)_5$ has a singlet ground state.[43] A similar spin change, occurring on ligand addition, is consistent with existing data for rate constants for the addition of CO and olefin to $Fe(CO)_3$(olefin).[47] Such a spin change is expected to lead to a highly constrained transition state.[17]

As with the $Fe(CO)_3(olefin)_2$ system, the analogous k_d for the loss of olefin from $Cr(CO)_5$(olefin) increases with olefin size and has been attributed to an increasing A factor[48] that can be related to the entropy of activation, $\Delta S^{\ddagger}$, using transition state theory.[38] An increasing and positive $\Delta S^{\ddagger}$ reflects the release of a larger number of degrees of freedom in the larger olefin that results from scission of the metal−olefin bond in $Cr(CO)_5$(olefin).[48] In addition to the overall entropies for the addition of olefin to $Fe(CO)_3$(olefin) for olefin = propene and that for 1-pentene determined in the present study, Table 2 also includes calculated entropies for the addition of C_2H_4 to $Fe(CO)_3(C_2H_4)$ and to $Cr(CO)_5$ using literature data for necessary rate constants.[28,47] The A factor for loss of olefin from $Fe(CO)_3(C_3H_6)_2$ was not determined in the study in ref 16. Rather, the A factor for the process was estimated based on the A factor for the corresponding process for $Fe(CO)_3(C_2H_4)_2$.

The thermochemical parameters associated with the equilibria in Scheme 2 can be presented in the form of a two-dimensional potential energy surface. Figure 8 shows such a potential energy surface for the enthalpies of the relevant species. The value determined for the enthalpy difference for $Fe(CO)_3(\eta^2$-pentene) relative to that for $HFe(CO)_3(\eta^3$-$C_5H_9)$ has been rounded to 10 kcal/mol and indicated as an approximate value as a consequence of the previously mentioned uncertainties inherent in this value. It is interesting to note that by considering the enthalpy alone (Figure 8), the lower energy of the minima of $Fe(CO)_3(\eta^2$-pentene$)_2$ relative to that for $HFe(CO)_3(\eta^3$-$C_5H_9)$ would significantly favor the former species. However, an analogous potential energy surface for the free energy shows

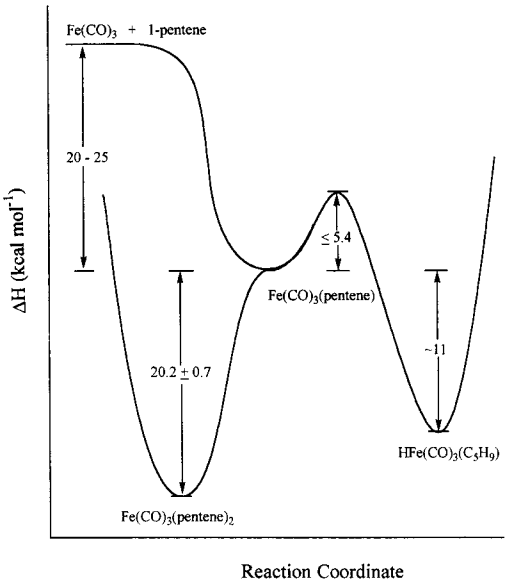

Figure 8. A two-dimensional representation of a proposed potential energy surface for the enthalpy in the $Fe(CO)_5$/1-pentene system.

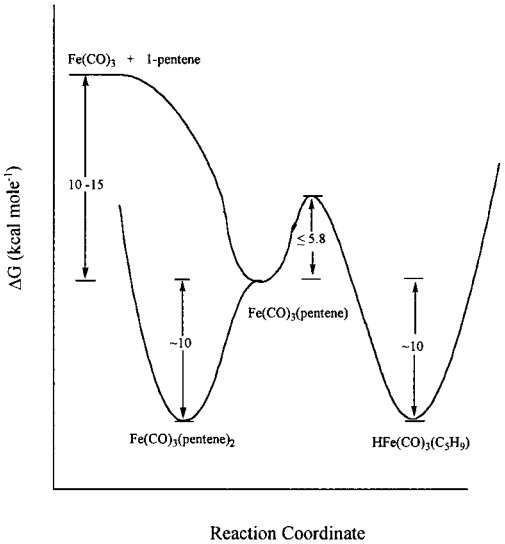

Figure 9. A two-dimensional representation of a proposed potential energy surface for the free energy in the $Fe(CO)_5$/1-pentene system.

the potential wells of $HFe(CO)_3(\eta^3$-$C_5H_9)$ and $Fe(CO)_3(\eta^2$-pentene$)_2$ to be more nearly even in energy (Figure 9). Though again the values for the free energy differences have been rounded as a consequence of the uncertainties inherent in the determination of these values, it is still quite clear that the entropy contributes significantly to the free energy to partially offset the enthalpic contribution associated with ligand addition to $Fe(CO)_3(\eta^2$-pentene).

F. Implications for Iron Carbonyl-Catalyzed Isomerization of Olefins. Previous studies of iron carbonyl-catalyzed olefin isomerization in both solution[11] and the gas phase[15] have shown that pulsed laser photolysis can generate a thermally

(48) (a) McNamara, B.; Becher, D. M.; Towns, M. H.; Grant, E. R. *J. Phys. Chem.* **1994**, *98*, 4622. (b) McNamara, B.; Towns, M. H.; Grant, E. R. *J. Am. Chem. Soc.* **1995**, *117*, 12254.

Scheme 4

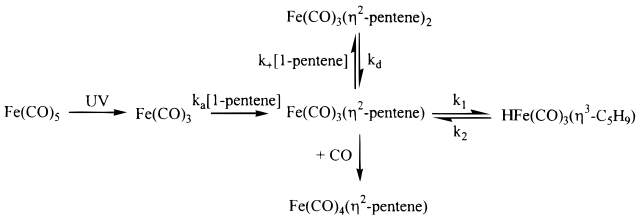

active catalyst at ambient temperatures. This catalyst, though it was not directly observed, was reported to have a lifetime on the order of $t \sim 0.2$ s,[11,15] with turnover numbers of several thousand per second. The observed behavior of both propene and 1-pentene as substrates is consistent with the proposed catalytic cycle shown in Scheme 1.

In each system, the lifetime of the $Fe(CO)_3(olefin)_2$ complex is on the order of at least hundreds of milliseconds in the presence of excess olefin. In the context of Scheme 1, this observation implicates $Fe(CO)_3(olefin)_2$ as the catalytic "reservoir" species. The lability of the olefin in $Fe(CO)_3(olefin)_2$, which provides a source of $Fe(CO)_3(olefin)$, is necessary for efficient substrate turnover in the catalytic cycle.

V. Conclusions

Scheme 4 presents an overview of the mechanism for isomerization of 1-pentene formulated as a result of this study. The processes in this mechanism occur on three distinct time scales. On the microsecond time scale, $HFe(CO)_3(\eta^3\text{-}C_5H_9)$ forms by a two-step process. When $Fe(CO)_3$ is generated by 308-nm gas-phase photolysis of $Fe(CO)_5$ in the presence of 1-pentene, the 1-pentene adds to $Fe(CO)_3$ to form $Fe(CO)_3(\eta^2\text{-}1\text{-pentene})$ with a bimolecular rate constant of $k_a = (4 \pm 1) \times 10^{-10}$ cm^3 molecule^{-1} s^{-1}. Rapid β-hydrogen transfer, by way of intramolecular C−H bond insertion to form $HFe(CO)_3(\eta^3\text{-}C_5H_9)$, follows rate-limited addition of 1-pentene to $Fe(CO)_3$ and proceeds with a lower bound of $k_1 \geq 10^9$ s^{-1}. Assuming a preexponential factor of $A = 10^{13}$ s^{-1},[16] an upper bound of $E_a \leq 5.4$ kcal mol^{-1} can be determined for the barrier to β-hydrogen transfer. At readily accessible pressures of 1-pentene, $HFe(CO)_3(\eta^3\text{-}C_5H_9)$ decays on a millisecond time scale with concurrent formation of $Fe(CO)_3(\eta^2\text{-pentene})_2$, by way of an $Fe(CO)_3(\eta^2\text{-pentene})$ intermediate. This decay occurs as a result of an equilibrium established between $HFe(CO)_3(\eta^3\text{-}C_5H_9)$ and $Fe(CO)_3(\eta^2\text{-pentene})$. It is $Fe(CO)_3(\eta^2\text{-pentene})$ that is in equilibrium with $HFe(CO)_3(\eta^3\text{-}C_5H_9)$ that adds 1-pentene to form $Fe(CO)_3(\eta^2\text{-pentene})_2$. The rate of the formation of $Fe(CO)_3(\eta^2\text{-pentene})_2$, shown in eq 13, is independent of 1-pentene pressure over the experimentally accessible pressure range. The behavior of the $Fe(CO)_5$/1-pentene system can be contrasted with the $Fe(CO)_5$/propene system, both of which can be described by a common set of kinetic equations. However, for propene the formation of $Fe(CO)_3(\eta^2\text{-}C_3H_6)_2$ is dependent on the propene pressure with a rate that is equal to $K_{eq}k_+[C_3H_6]$. This difference in behavior is attributed to an equilibrium constant that is shifted by ~3 orders of magnitude toward $HFe(CO)_3(\pi\text{-allyl})$ for 1-pentene relative to propene. This shift leads to the dominance of the pressure-independent term (k_d) in eq 13 for pentene, while for propene the pressure-dependent term is dominant. Hence, for the 1-pentene system the rate of formation of the bisolefin adduct is equal to $k_d \sim 20$ s^{-1}, where k_d is the unimolecular rate constant *for loss* of 1-pentene from $Fe(CO)_3(\eta^2\text{-pentene})_2$. The change in the magnitude of the equilibrium constant between the two systems implies a ~4 kcal mol^{-1} enthalpy difference between $HFe(CO)_3(\eta^3\text{-allyl})$ and $Fe(CO)_3(\eta^2\text{-olefin})$ for 1-pentene as the starting olefin relative to propene. CO may add to $Fe(CO)_3(\eta^2\text{-pentene})$ that is in equilibrium with $HFe(CO)_3(\eta^3\text{-}C_5H_9)$ to form $Fe(CO)_4(\eta^2\text{-pentene})$. $Fe(CO)_4(\eta^2\text{-pentene})$ remains stable on the time scale of catalytic turnover and its formation serves as a termination pathway for thermal catalysis.

This study has a number of important implications for the generally accepted mechanism for transition metal catalyzed olefin isomerization which is shown in Scheme 1 and strongly supported by the results of this study and a prior study on intermediates formed by the interaction of propene with $Fe(CO)_3$.[16] Data are now available on both the rate constants and the thermochemistry for the principal steps in this mechanism for both this system and the propene system. Differences in the kinetics and thermodynamics between these systems result principally from the differences in magnitude of the equilibrium constant for the $HFe(CO)_3(\eta^3\text{-allyl}) \rightleftarrows Fe(CO)_3(\eta^2\text{-olefin})$ equilibrium. The source of the difference in these equilibrium constants is not yet clear but is of interest for future investigations. Future studies should help elucidate the generality of the kinetic model (eqs 1−4) for the iron carbonyl induced isomerization of olefins. The data from this study and the prior study of the propene system[16] both strongly implicate the bisolefin species as the "catalytic reservoir" species because the lability of the bound olefin can generate $Fe(CO)_3(olefin)$, which is required for efficient catalytic turnover.

Acknowledgment. We acknowledge support of this work by the National Science Foundation under grants CHE90-24509 and CHE97-34891. We thank one of the referees for pointing out a simplification of our original derivation of eq 10.

JA9914341